Electronic Supplementary Information

Theoretical probing monolayer BiI_3 as electrolyte separator and 3*d*-TM doped BiI_3 as electrocatalysts toward high performance Lithium-Sulfur batteries

Wentao Wu[a], Kaixin Zou[a], Li Wang[a,b], Boyan Li[*,c],Wen Yang[d], Chunlai Gao[e], Feng Lu[*,a], Weichao Wang[a], Wei-Hua Wang[*,a]

[a]Department of Electronic Science and Engineering, and Tianjin Key Laboratory of Efficient Utilization of Solar Energy, Nankai University, Tianjin 300350, China

[b]Nanoyang Group, State Key Laboratory of Chemical Engineering, School of Chemical Engineering and Technology, Tianjin University, Tianjin, 300072, China

[c]National Institute of Clean-and-Low-Carbon Energy and Beijing Engineering Research Center of Nano-structured Thin Film Solar Cells, Beijing 102211, China

[d]Shanxi Key Laboratory of Metal Forming Theory and Technology, School of Material Science and Engineering, Taiyuan University of Science and Technology, Taiyuan 030024, China

[e]Faculty of Mathematics and Physics, Huaiyin Institute of Technology, Huaian 223001, China

*Email: whwangnk@nankai.edu.cn, boyan.li.a@chnenergy.com.cn, lufeng@nankai.edu.cn

Details of formation energy of the substitutional doping configuration (TM_{sub}/BiI_3)

The formation energy of substitutional doping for TM_{sub}/BiI_3 is expressed as,

$$E_{form} = E_{TM_{sub}/BiI_3} + E_{Bi} - E_{BiI_3} - E_{TM}$$

where E_{TM_{sub}/BiI_3}, E_{BiI_3}, E_{TM} and E_{Bi} are the energies of the substitutional doping systems, the monolayer BiI_3 supercell, one single TM and Bi atom, respectively.

Details of equilibrium potential (U_{eq}) of Sulfur reduction reaction

The computational details are analogous to the oxygen reduction reaction and oxygen evolution reaction processes. Firstly, the stander free energy of Li_2S formation is defined by the following formula,

$$\Delta G_f^0 = 8G(Li_2S_{bulk})^0 - G(S_{8\text{ - bulk}})^0 - 16G(Li_{atom})^0$$

where $G(Li_2S_{bulk})^0$, $G(S_{8\text{ - bulk}})^0$, $G(Li_{atom})^0$ represent the total energies of bulk Li_2S, one S_8 cluster, and one Li atom in bulk phase. Here, the Gibbs energy of Li_2S, S_8 are -32.918 eV, -11.995 eV, respectively. Therefore, the stander free energy of Li_2S formation (ΔG_f^0) and equilibrium potential are calculated as follows,

$$\Delta G_f^0 = -32.546 \text{ eV}$$

$$U_{eq} = -\frac{\Delta G_f^0}{16e} = \frac{32.546 \text{ eV}}{16e} = 2.034 \text{ V}$$

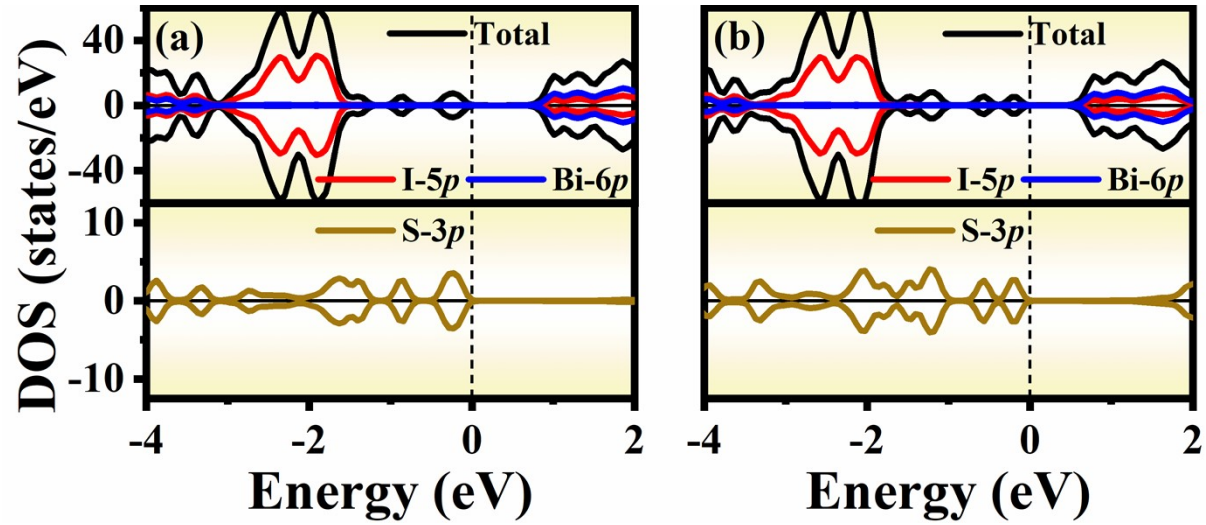

Fig. S1 Density of states for monolayer BiI_3 adsorbed with Li_2S_6 in (a) and with Li_2S_8 in (b).

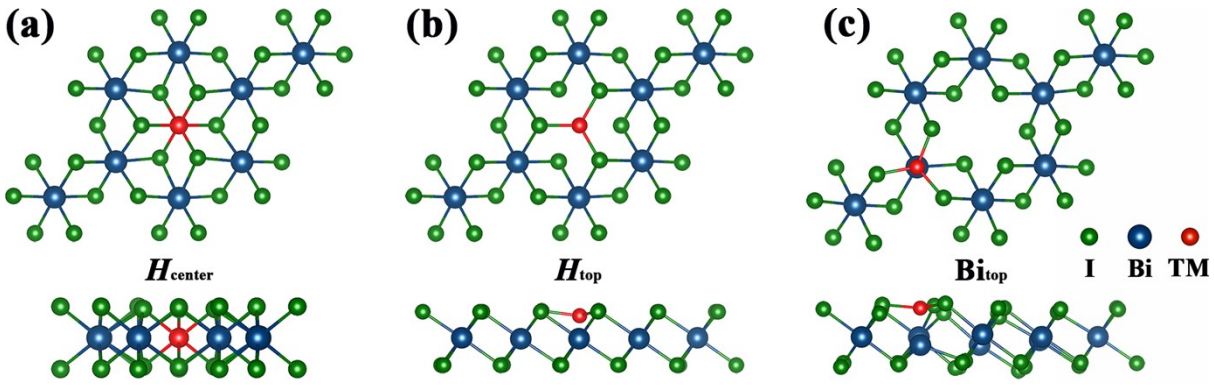

Fig. S2 The three stable adsorption doping configurations of 2D TM/BiI_3 with the H_{center} configuration for Ti, V, Cr, Mn/BiI_3 systems in (a), H_{top} configuration for Cu/BiI_3 system in (b), Bi_{top} configuration for Fe, Co, Ni/BiI_3 systems in (c).

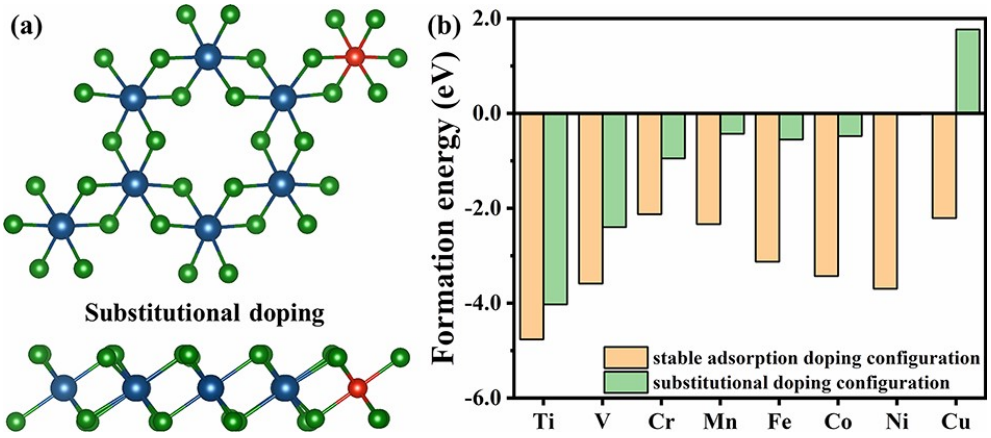

Fig. S3 (a) Top view and side view of the substitutional doping TM_{sub}/BiI_3 systems, and formation energies of the most stable adsorption doping TM/BiI_3 systems and the substitutional doping TM_{sub}/BiI_3 systems in (b).

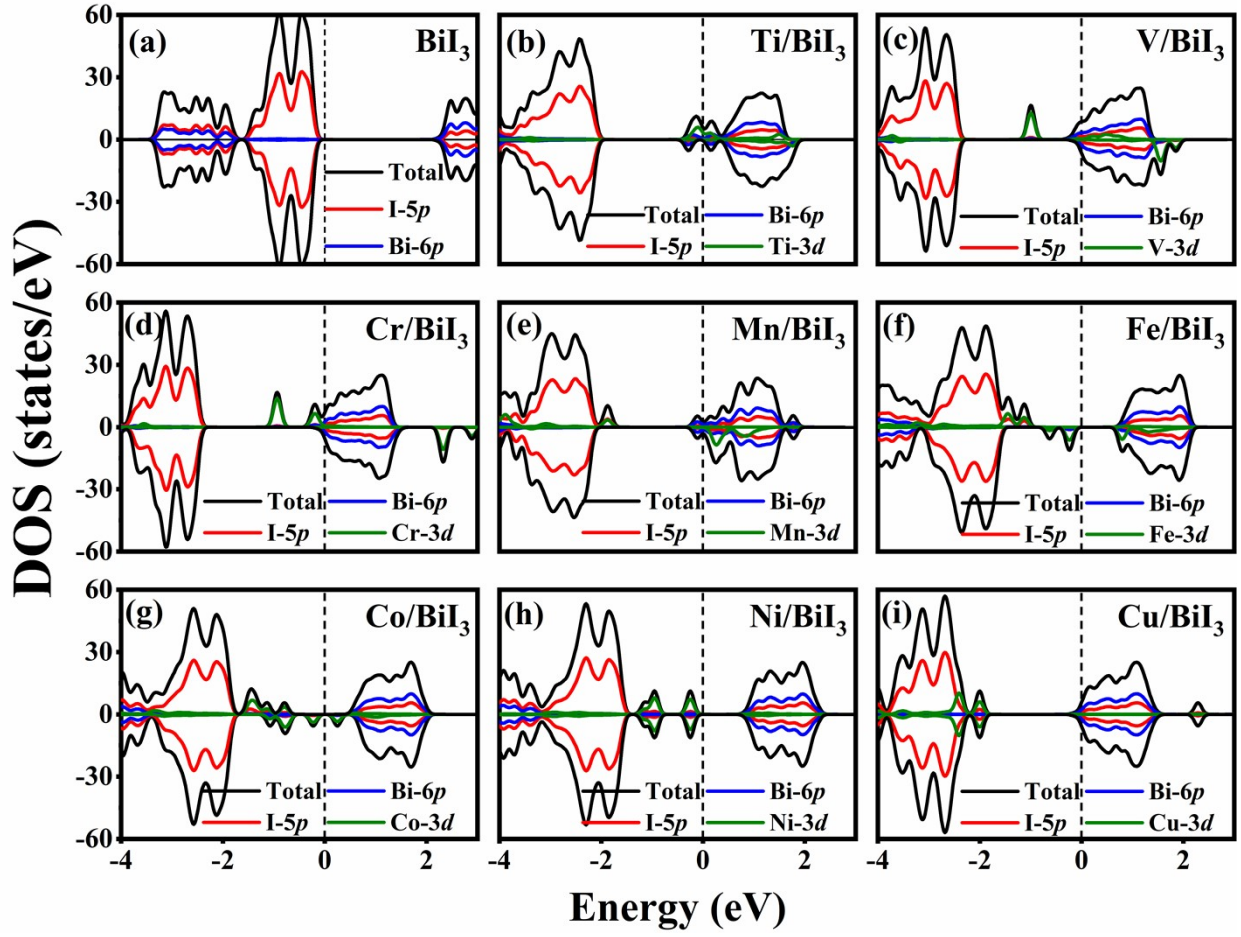

Fig. S4 Density of states for (a) pristine BiI_3 and (b-i) 3*d*-TM/BiI_3 systems. (b) Ti/BiI_3, (c) V/BiI_3, (d) Cr/BiI_3, (e) Mn/BiI_3, (f) Fe/BiI_3, (g) Co/BiI_3, (h) Ni/BiI_3, (i) Cu/BiI_3.

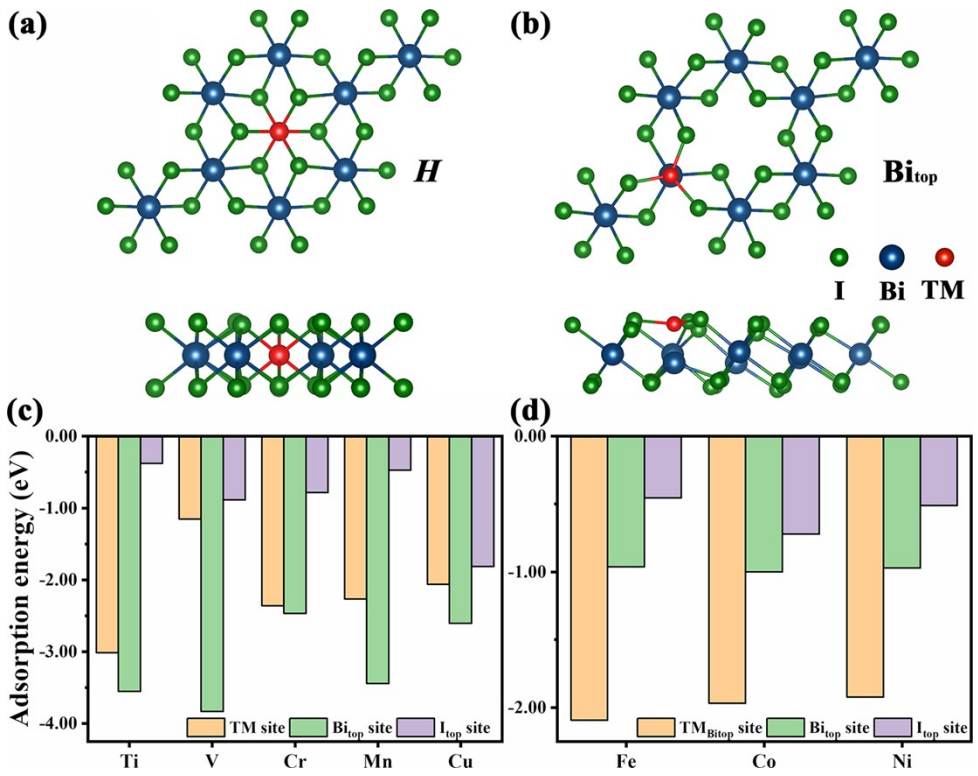

Fig. S5 (a) Top view and side view of LiPSs adsorption sites on *H* doped site (Ti, V, Cr, Mn, Cu doped BiI_3) (b) and Bi_{top} doped site (Fe, Co, Ni doped BiI_3) configurations, respectively. Adsorption energies of Li_2S at different adsorption sites for *H* doped site configuration (Ti, V, Cr, Mn, Cu doped BiI_3) in (c) and on Bi_{top} doped site configuration (Fe, Co, Ni doped BiI_3) in (d).

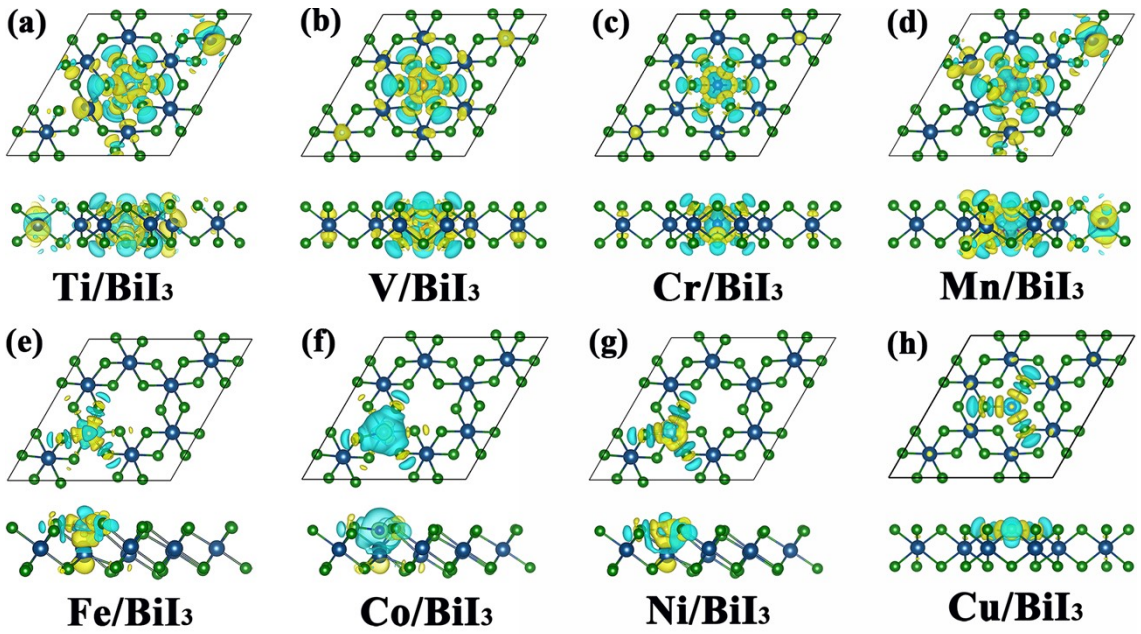

Fig. S6 Charge density difference in top and side views for (a) Ti/BiI_3, (b) V/BiI_3, (c) Cr/BiI_3, (d) Mn/BiI_3, (e) Fe/BiI_3, (f) Co/BiI_3, (g) Ni/BiI_3, (h) Cu/BiI_3 systems.

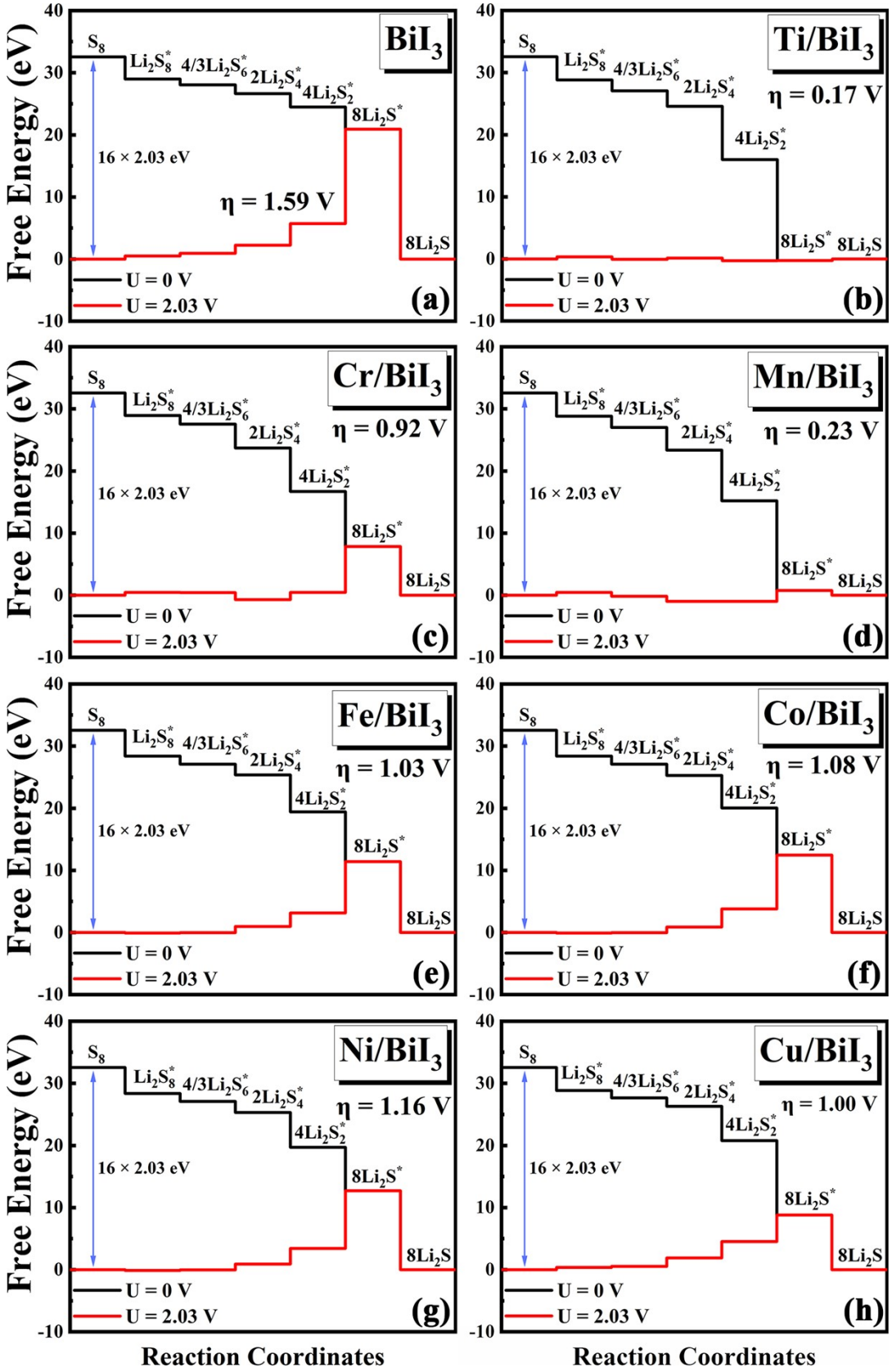

Fig. S7 Free energy of SRR for TM/BiI_3 systems at U = 0 V and equilibrium potential (U = 2.03V).

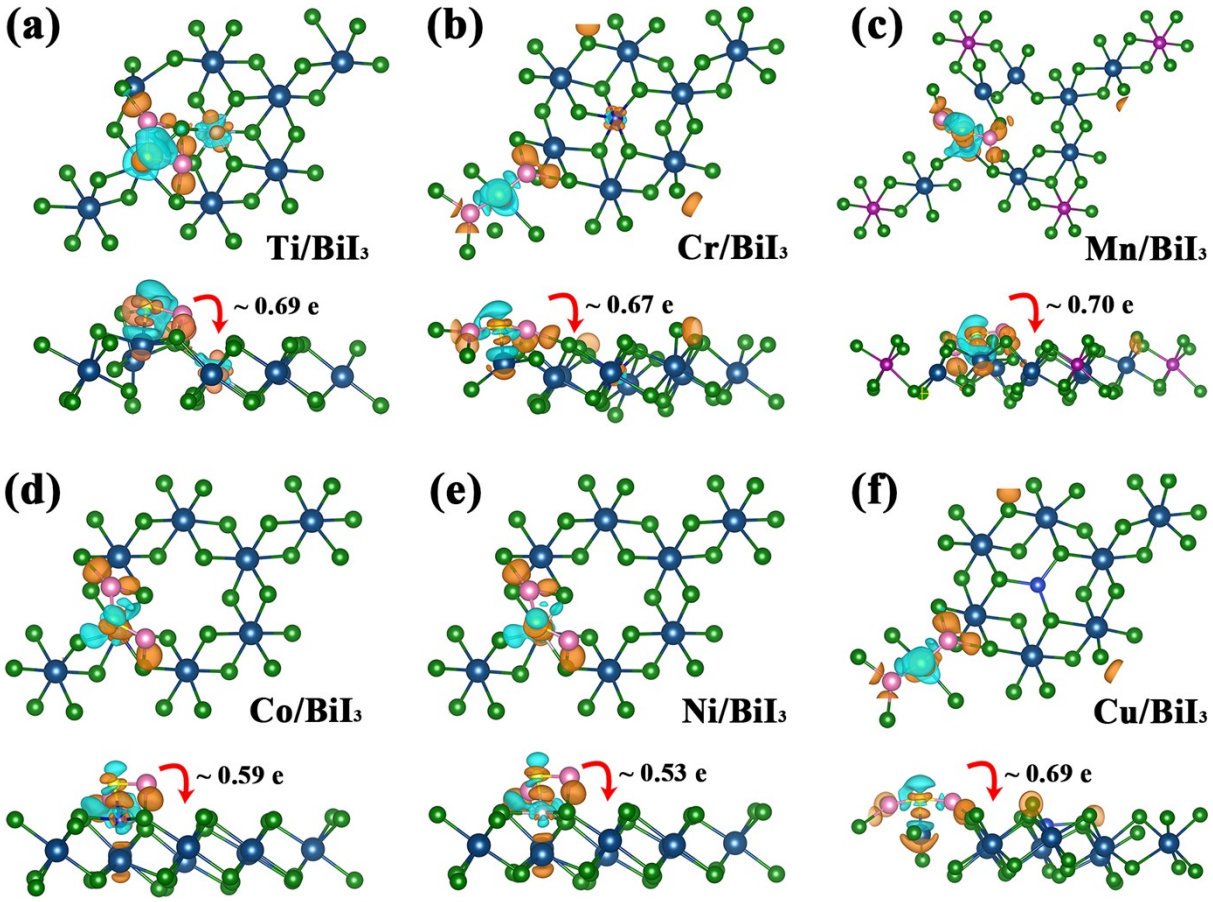

Fig. S8 Charge density difference in top and side views for Li_2S adsorbed on (a) Ti/BiI_3, (b) Cr/BiI_3, (c) Mn/BiI_3, (d) Co/BiI_3, (e) Ni/BiI_3, (f) Cu/BiI_3 systems.

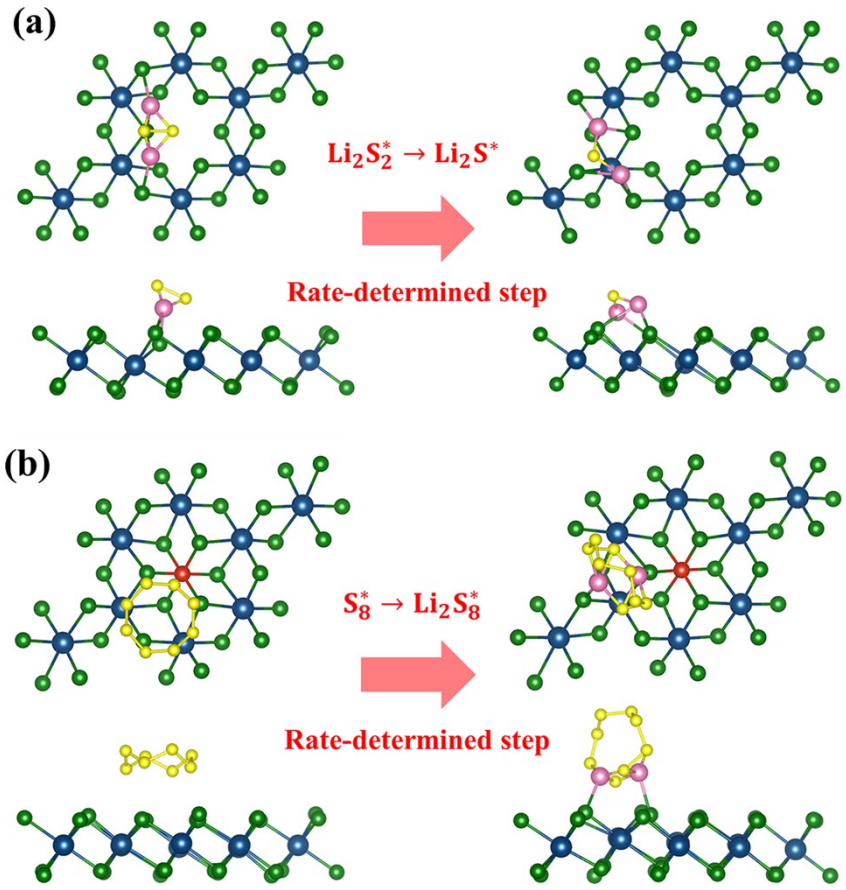

Fig. S9 The diagrams of rate-determined step on BiI_3 (a) and V/BiI_3 in (b).

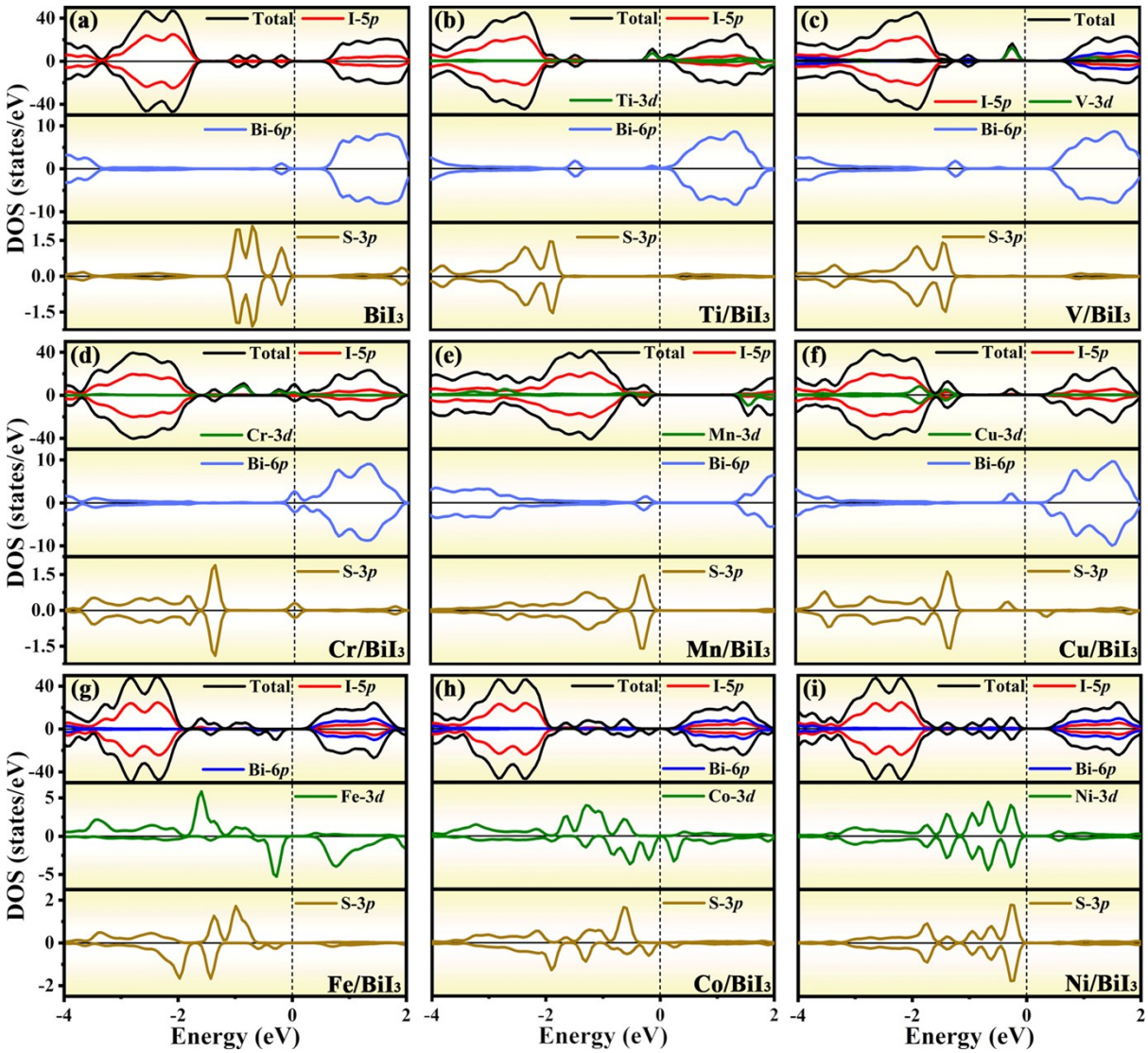

Fig. S10 Density of states of Li_2S adsorbed on BiI_3 in (a), Ti/BiI_3 in (b), V/BiI_3 in (c), Cr/BiI_3 in (d), Mn/BiI_3 in (e), Cu/BiI_3 in (f), Fe/BiI_3 in (g), Co/BiI_3 in (h) and Ni/BiI_3 in (i).

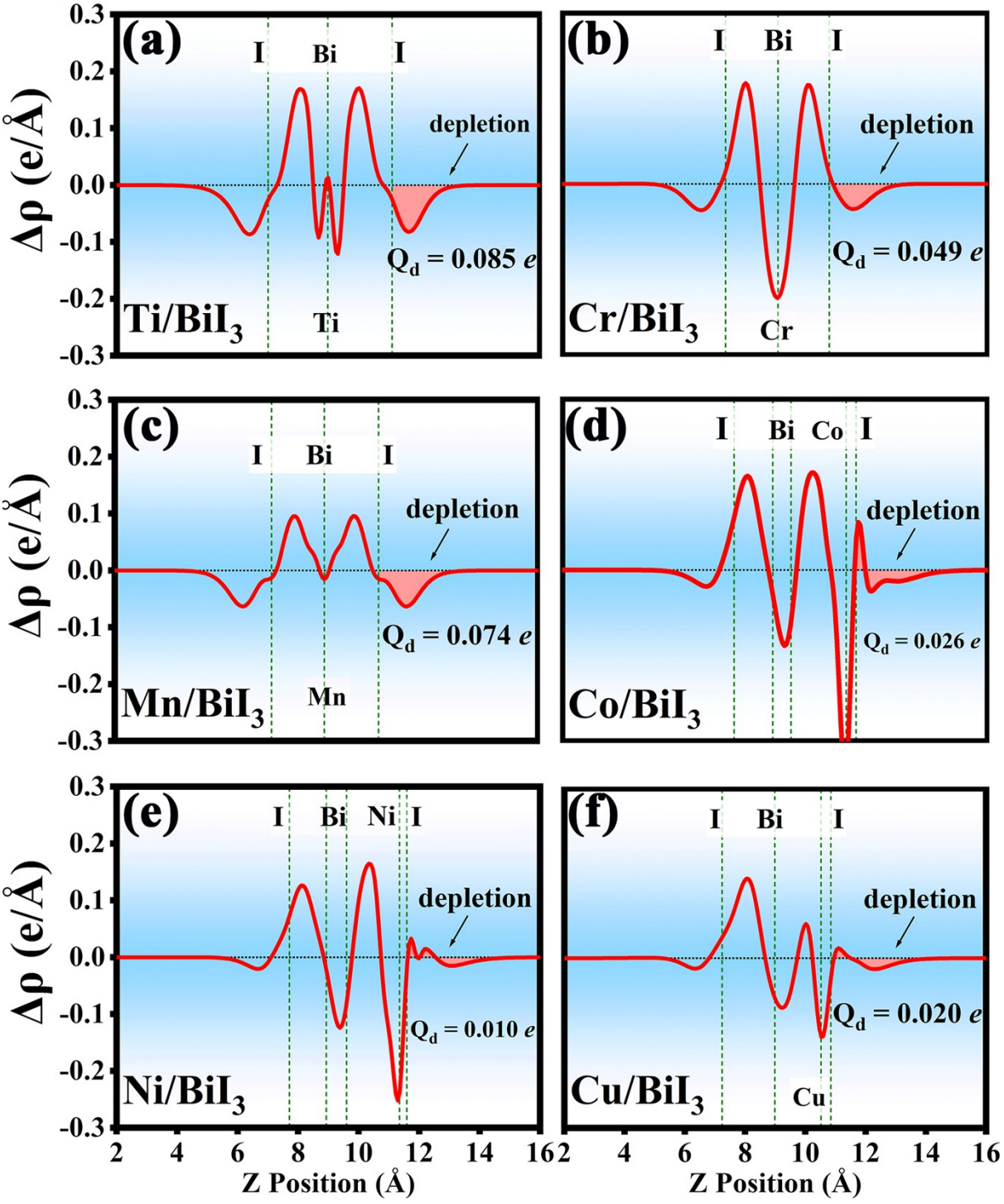

Fig. S11 The xy plane-averaged charge density differences along the z axis for (a) Ti/BiI3, (b) Cr/BiI3, (c) Mn/BiI3, (d) Co/BiI3, (e) Ni/BiI3, and (f) Cu/BiI3 systems.

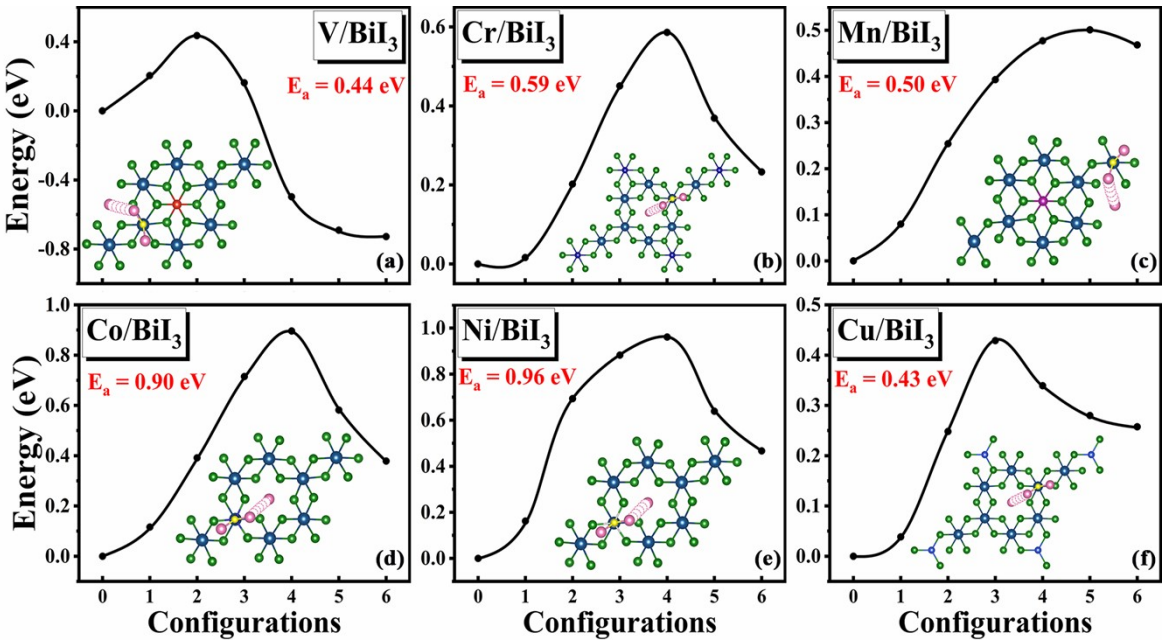

Fig. S12 Li_2S decomposition barrier curves for (a) V/BiI_3, (b) Cr/BiI_3, (c) Mn/BiI_3, (d) Co/BiI_3, (e) Ni/BiI_3, (f) Cu/BiI_3 systems.

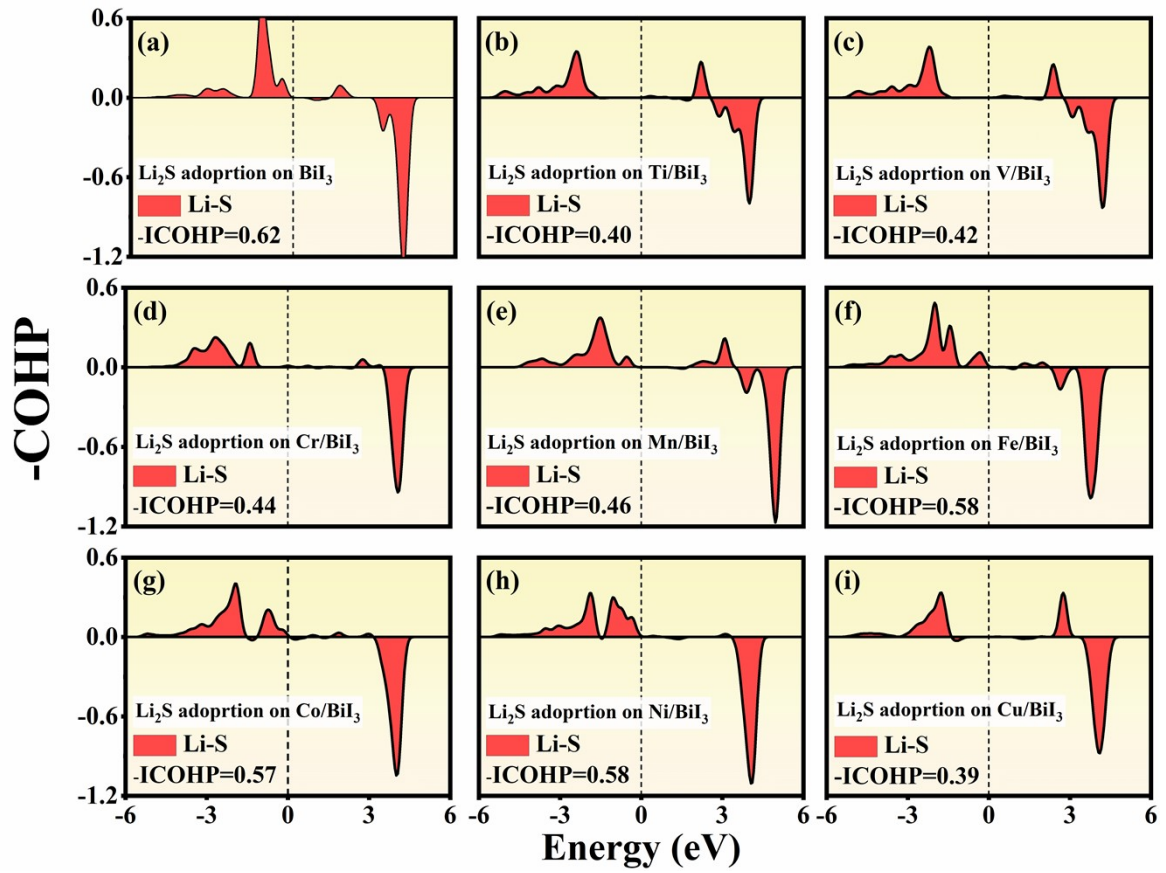

Fig. S13 The COHP of Li-S bonds in Li_2S adsorbed on 3*d*-TM doped BiI_3 systems. (a) BiI_3, (b) Ti/BiI_3, (c) V/BiI_3, (d) Cr/BiI_3, (e) Mn/BiI_3, (f) Fe/BiI_3, (g) Co/BiI_3, (h) Ni/BiI_3, (i) Cu/BiI_3.